

## **Stereolithography Cure Process Modeling Using Acrylate Resin**

Yanyan Tang<sup>†</sup>, Clifford L. Henderson<sup>†</sup>, John Muzzy<sup>†</sup>, David W. Rosen\*

<sup>†</sup> School of Chemical & Biomolecular Engineering, 311 Ferst Drive, N.W., Georgia Institute of Technology, Atlanta, GA 30332-0100

\*Corresponding author; School of Mechanical Engineering, 813 Ferst Drive, N.W., Georgia Institute of Technology, Atlanta, GA 30332-0405; Email: david.rosen@me.gatech.edu

Reviewed, accepted September 1, 2004

### **Abstract**

In this paper, a complex stereolithography (SL) cure process model is presented that incorporates transient thermal and chemical effects which influence final part shape and properties. The model incorporates photopolymerization, mass diffusion, and heat transfer. Material properties are characterized and a comprehensive kinetic model parameterized for a model compound system. SL process simulations are performed using finite element methods with the software package FEMLAB, and validated by the capability of predicting the fabricated part dimensions. A degree of cure (DOC) threshold model is proposed which can predict the cure line size within 15% error, comparing with 30% prediction error by the exposure threshold model currently used in SL. Furthermore, through the sensitivity analysis conducted by the process model presented here, the sensitive parameters are identified and the SL bath temperature, photoinitiator absorptivity and concentration are found to be the most sensitive factors that affect the SL fabrication results. The sensitive variables will be the focus of further research meant to improve SL process speed and resolution.

### **Introduction**

In the stereolithography (SL) process, parts are fabricated in a layer-by-layer manner by curing photopolymer resins with a UV laser. For some applications, the SL process requires improvements in speed and resolution, but it is not clear that both can be improved simultaneously. A better understanding of the SL process is needed in order to improve the technology. Being able to simulate and predict part shape, build time, and potential difficulties would be very beneficial. To accomplish this, a more complete model of SL cure is needed [1]. Furthermore, improvements to SL machines can be investigated to determine their impact on building speed, resolution, and other concerns.

Current models of the SL process assume that the extent of resin curing is a function of only the amount of exposure to UV radiation [2]. They utilize a threshold model that assumes a dose  $E(x,y,z)$  that is greater than a minimum "critical exposure,"  $E_c$ , causes the resin to solidify at point  $(x,y,z)$ . This is a gross oversimplification of the process that ignores important transient, thermal, and chemical effects. SL cure is a time-varying process that is governed by complex, exothermic chemical reactions that have multiple reaction pathways. A more complete model is needed that accounts for these effects.

In this paper, a more complex SL cure model is presented that captures effects that are ignored in the threshold model. It incorporates heat transfer, mass transfer, and reaction kinetics, and thus simulates the variation of temperature and material properties during the SL curing process. It is important to model the transient 3-D distribution of temperature, since temperature influences reaction rates and, if high enough, can cause thermal curing. With the SL cure model presented here, it is possible to investigate the spatial and temporal distributions of monomer and polymer concentrations, molecular weight, cross-link density, and degree of cure, which are necessary to characterize the cured part. This paper presents that the size of the cured part can be predicted from the monomer conversion profile.

The SL cure model is formulated as a set of partial differential equations, with initial conditions specified based on the chemistry and physics of laser exposure and photoinitiation. This model is then solved using the finite element method with the software package FEMLAB. Numerical results are compared with experimental measurements and it is shown that from the degree of cure profile, the cured part size upon variation of process or material parameters can be predicted.

### Model Development

The simplest case of complex laser drawing patterns in SL apparatus is that the laser moves along one direction and draws a single vector scan line. The cured shape upon a single laser drawn line is a parabolic cylinder [1], as shown in Figure 1, where the x axis is the laser drawing direction. Considering the repetition of the parabolic plane along the x axis and its symmetry about the x-z plane, a rectangular domain in Cartesian coordinates (Figure 2) was established to simulate the resin cure behaviour during the single-line drawing process. The shaded region is where the temperature or concentrations vary, the size of which increases with time as heat conduction and/or molecular diffusion continues [3]. The domain is chosen to be large enough to ensure ambient temperature and concentrations outside the rectangle at any time.

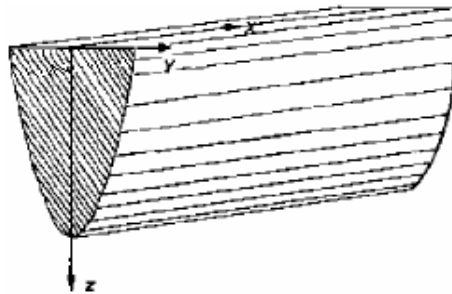


Figure 1 SL cured shape upon a single laser drawn line

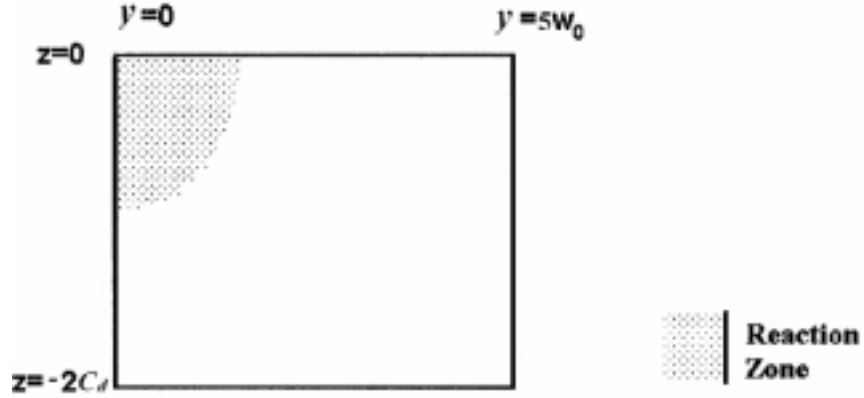


Figure 2 SL process modelling domain for single laser drawn line

Mass transfer by diffusion and heat transfer by conduction are the two transport phenomena occurring in the SL cure process. Equations (1)-(3) describe the energy balance, mass balance for monomer, and mass balance for the polymeric radicals (including monomer radicals), respectively.

$$\rho C_p \frac{\partial T}{\partial t} = k \left\{ \frac{\partial^2 T}{\partial x^2} + \frac{\partial^2 T}{\partial y^2} + \frac{\partial^2 T}{\partial z^2} \right\} + \Delta H_p R_p \quad (1)$$

$$\frac{\partial [M]}{\partial t} = D_M \left\{ \frac{\partial^2 [M]}{\partial x^2} + \frac{\partial^2 [M]}{\partial y^2} + \frac{\partial^2 [M]}{\partial z^2} \right\} + (-R_p) \quad (2)$$

$$\frac{\partial [P\bullet]}{\partial t} = D_{P\bullet} \left\{ \frac{\partial^2 [P\bullet]}{\partial x^2} + \frac{\partial^2 [P\bullet]}{\partial y^2} + \frac{\partial^2 [P\bullet]}{\partial z^2} \right\} + (-R_t) \quad (3)$$

The source terms  $\Delta H_p R_p$ ,  $-R_p$ , and  $-R_t$  are dependent on the photopolymerization kinetics of the resin, which will be discussed later. The terms containing x variations can be removed neglecting property variations in the scanning direction (x axis). The corresponding initial and boundary conditions are as follows:

$$\begin{aligned} [Q] &= [Q]_i & \text{at } t = 0, 0 \leq y \leq 5w_0, -2C_d \leq z \leq 0 & \quad (a) \\ \frac{\partial Q}{\partial y} &= 0 & \text{at } y = 0, -2C_d \leq z \leq 0, t \geq 0 & \quad (b) \\ [Q] &= [Q]_0 & \text{at } y = 5w_0, -2C_d \leq z \leq 0, t \geq 0 & \quad (c) \\ \frac{\partial Q}{\partial z} &= 0 & \text{at } z = 0, 0 \leq y \leq 5w_0, t \geq 0 & \quad (d) \\ [Q] &= [Q]_0 & \text{at } z = -2C_d, 0 \leq y \leq 5w_0, t \geq 0 & \quad (e) \end{aligned} \quad (4)$$

where  $Q$  represents  $T$ ,  $[M]$ , or  $[P\bullet]$ ,  $C_d$  is the cure depth, maximum depth of the polymerized area, and  $w_0$  is the laser beam radius. The domain size can be initially set based on the  $C_d$  and  $w_0$  values and adjusted later according to the simulation results. Note that for both temperature and

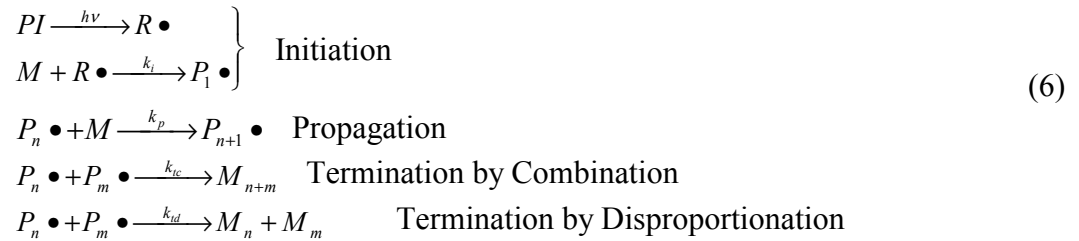
monomer concentration,  $[Q]_i = [Q]_0$ , but for radical concentration,  $[Q]_0 = 0$  and  $[Q]_i \neq [Q]_0$ , where  $[Q]_i$  will be addressed soon. For the temperature condition at  $z=0$  boundary, heat transfer with the natural air environment was considered, and thus temperature condition (d) in Equation (4) becomes:

$$k \frac{\partial T}{\partial z} = h(T_{\text{inf}} - T) \quad \text{at } z = 0, 0 \leq y \leq 5w_0, t \geq 0 \quad (5)$$

where  $h$  is the heat transfer coefficient at the resin surface in the SL machine chamber, and  $T_{\text{inf}}$  is the environmental temperature in the SL machine chamber.

### Photopolymerization Kinetic Model

As mentioned earlier, all source terms in the balance equations are related to the kinetics of the resin polymerization. The photocure kinetics of the resin therefore needs to be characterized. The mechanism of radical photopolymerization can be briefly described as follows:



where  $PI$  represents the photoinitiator, which decays to generate primary radicals  $[R \bullet]$ ;  $M$  stands for monomer, which reacts with radicals to create and elongate polymer chains  $P_n \bullet$ ; these chain radicals  $P_n \bullet$  could combine with one another and terminate to become dead polymer  $M_n$ , which is no longer reactive.

Corresponding to the reaction mechanism, the rates of the initiation, propagation and termination reactions are expressed as Equations (7), (8) and (9), respectively.

$$R_i = \phi_i I_a \quad (7)$$

$$R_p = k_p [P \bullet] [M] \quad (8)$$

$$R_t = k_t [P \bullet]^2 \quad (9)$$

where  $\phi_i$  is the initiation quantum yield,  $I_a$  is the absorbed light intensity ( $\text{mol}/\text{m}^3\text{-s}$ ),  $[P \bullet]$  is the chain radical concentration,  $[M]$  is the monomer concentration, and  $k_p$  and  $k_t$  are the propagation and termination rate constants, respectively. The dependence of  $k_p$  and  $k_t$  on temperature and free volume can be incorporated into one equation [4,5]:

$$k_p = \frac{k_{p0}}{1 + e^{A_p(1/f - 1/f_p)}} \quad (10)$$

$$k_t = \frac{k_{t0}}{1 + \frac{R_{rd} k_p [M] / k_{t0} + e^{-A_t(1/f-1/f_{ct})}}{k_{p0}}} \quad (11)$$

where  $f$  is the fractional free volume,  $f_{cp}$  and  $f_{ct}$  are critical fractional free volume terms for propagation and termination, respectively,  $R_{rd}$  is reaction diffusion parameter [4,5];  $k_{p0}$  and  $k_{t0}$ , dependent on temperature, are the rate constants when the reactions are not limited by diffusion;  $A_p$  and  $A_t$  are temperature-independent constants to be determined by fitting the experimental data.

The initial radical concentration is obtained by integrating the rate of initiation:

$$[P\bullet]_0 = \phi_i S_0 (1 - e^{-2.3\epsilon E}) \quad (12)$$

where  $\epsilon$  and  $S_0$  are the absorption coefficient and initial concentration of initiator, respectively, and  $E$  ( $\text{mol/m}^2$ ) is the exposure applied on the resin.

### *Model Parameters*

Table 1 lists all the parameters (except the kinetic ones which will be discussed later) that need to be determined for the model constructed by Equations (1)-(5). The process and laser parameters were obtained from the single line part building process in a SLA-250 machine (3D Systems). The material properties were based on the model compound system comprised of SR@494 tetraacrylate (Sartomer) and photoinitiator Irgacure@651 (Ciba). The thermal conductivity and heat capacity of hexanedioldiacrylate (HDDA) [3] were adopted. The density of the curing material was approximated by taking the average of the densities of pure monomer and polymer. The heat of polymerization was calculated to be 346kJ/mol from the theoretical enthalpy of 20.6kcal/mol for the acrylate double bond [6]. The absorption coefficient of initiator was measured using UV-VIS spectrometer (Lambda 19, Perkin Elmer) and calculated according to Beer's law. The coefficients of thermal expansion of monomer and cured polymer were obtained by using an ellipsometer (VB250 VASE, J.A. Woollam) to measure the film thickness at elevated temperatures. The glass transition temperatures were measured from a differential scanning calorimeter (DSC2920, TA Instruments). The density of the cured polymer was measured using density gradient column (DC-4, Techne). For the material composition, 2wt% Irgacure@651 was added to the SR@494 acrylate.

### **Kinetic Experiments**

Representative of the acrylate compounds commonly used in the SL resins [10-13], ethoxylated (4) pentaerythritol tetraacrylate (E4PETeA, SR@494, Sartomer) was chosen as the model material to simulate the polymerization behaviour in the SL bath. 2,2-dimethoxy-2-phenylacetophenone (DMPA, Irgacure@651, Ciba) was used as the initiator for E4PETeA. E4PETeA was used after dehibition by a prepacked inhibitor remover column (Aldrich). 0.2wt% DMPA was added in the dehibited acrylate. 1.16( $\pm 0.05$ )mg sample was put in the aluminum pan

using micropipette to make about 0.13mm thickness. Such small amount of sample ensures a low attenuation (~5%) of the incident light, therefore, the light intensity and reaction inside the sample can be assumed uniform. The aluminum pans were machined specifically to have a 0.13mm depression to hold the sample by which the thickness uniformity can be assured [14]. The pans were also coated with carbon to reduce the aluminum reflection (the reflectance of aluminum is 0.9642 [15]) at the bottom and the standing waves consequently formed inside the sample. The DSC Q1000 with photo calorimetric accessory (PCA) (TA Instruments) was adopted to characterize the kinetics of the model acrylate resin. The light source Novacure 2100 (EXFO Photonic Solutions) was used with filtered wavelength at 365nm. The power that reached the sample was 0.06mW.

Table 1 Parameters used in the comprehensive SL process model

	<b>Parameter</b>	<b>Unit</b>	<b>Data Range</b>
Process Parameters	laser scanning velocity	m/s	0.0272
	bath temperature	K	304.65
	heat convection coefficient	W/m <sup>2</sup> -K	4.18 [7]
Laser Parameters	laser power	W	0.028
	Wavelength	nm	325
	beam radius	m	1.10E-04
Material Properties	thermal conductivity	W/m-K	0.2 [3]
	density	kg/m <sup>3</sup>	1175
	heat capacity	J/kg-K	1700 [3]
	heat of polymerization	J/mol	3.46E+05
	absorptivity(initiator)	m <sup>3</sup> /mol-m	19.9
	initiation quantum yield		0.6 [5]
	diffusion coefficient(monomer)	m <sup>2</sup> /s	1e-14 - 1e-8 [8]
	diffusion coefficient(radical)	m <sup>2</sup> /s	1e-14 - 1e-8 [8]
	coefficient of thermal expansion(monomer)	1/K	0.00182
	coefficient of thermal expansion(polymer)	1/K	0.00032
	glass transition temperature(monomer)	K	209.9
	glass transition temperature(polymer)	K	503.15
	density(monomer)	kg/m <sup>3</sup>	1128[9]
density(polymer)	kg/m <sup>3</sup>	1200	
Resin Compositions	monomer concentration	mol/m <sup>3</sup>	2136
	photoinitiator concentration	mol/m <sup>3</sup>	89.8

Both continuous and flash exposure experiments were carried out at three different temperatures (30, 50, 70°C). During continuous irradiation experiments, the light is on until the heat flow curve drops to the baseline, i.e. the reaction is complete under current temperature. The light turns on only for a relatively very short time in flash exposure experiments. For each temperature, 5 or more different flash times were used in order to capture the kinetic constants at different conversions. Applying quasi steady state assumption (QSSA) in the continuous irradiation experiments,  $k_p/k_t^{1/2}$  can be evaluated; from the flash exposure experiments,  $k_t/k_p$  can be determined from the slope of a plot of  $(1-X)/(dX/dt)$  as a function of time in the dark reaction region [14]. Thus the kinetic constants  $k_p$  and  $k_t$  are determined at 5 or more different conversions for each temperature, which contributes to the parameterization of  $k_p$  and  $k_t$  dependence on conversion or fractional free volume. Experiments performed at different temperatures complete the parameterization of temperature dependence of  $k_p$  and  $k_t$ .

In this study, instead of assuming QSSA in the continuous exposure case, the rate of radical concentration changing (Equation 13) was integrated to obtain the relationship of  $k_p$  and  $k_t$ . Trial and error was used to solve this relationship and the one from the dark reaction (Equation 14) simultaneously.  $k_p/k_t^{1/2}$  values thus obtained were about 20 or 30% different from those evaluated using QSSA for high conversions; there was less than 5% difference at low conversions ( $X < 25\%$ ), indicating QSSA is valid only at low conversions.

$$\frac{d[M\bullet]}{dt} = R_i - k_t[M\bullet]^2 \quad (13)$$

$$\frac{d[M\bullet]}{dt} = -k_t[M\bullet]^2 \quad (14)$$

### Simulations

The multiphysics modelling and simulation code FEMLAB was used as the simulation environment. FEMLAB is a product of the COMSOL Group [16] and has many model types available for use (application models). It also supports equation-based modelling, enabling users to enter their specific partial differential field equations. Application models were used for this research.

Since SL curing is a coupled mass and energy balance problem, two application models, diffusion and heat transfer by conduction, were employed in FEMLAB to complete the description of the model discussed in last section. The geometric domain being modelled is shown in Figure 2. As mentioned earlier, a small size for the domain is chosen initially, which is then increased until no significant deviation in the modeling results obtained from larger domain sizes is observed. Balance equations (1)-(3) are consistent with the “Subdomain Settings” for the two transient application modes; initial conditions Equation (4a) are entered here also. Equations (4b-e) correspond to the “Boundary Settings”.  $k_p$  and  $k_t$  models along with other expressions such as  $R_p$ ,  $R_t$  and fractional free volume enter the “Expressions”, and all related parameters as listed in Table 1 are entered under the “Constants” option. Triangular, quadratic, Lagrange elements were selected for domain discretization. The mesh at the left upper corner, where most property variations occur, was refined. The problem was then solved by a time dependent solver in the software. Absolute and relative tolerances for time step size determination were 0.1 ( $10^{-6}$  for radical concentration) and 0.01, respectively.

Three cases cover the basic processes in SL: single-scan-single-layer (Figure 1), multiple-scan-single-layer with certain hatching space between neighboring lines, and single-scan-multiple-layer (stack of single scans). Only the single line case (Figure 1) was simulated here. The other two simulations for methyl methacrylate were discussed in [17].

Similarly to the previous observations [17], the curing reaction occurs immediately upon the laser exposure (Figures 3). The radical population is significantly exhausted and the temperature increases by approximately  $10^\circ\text{C}$  during the first 0.1sec. The monomer is consumed significantly in the first 0.1s as well.

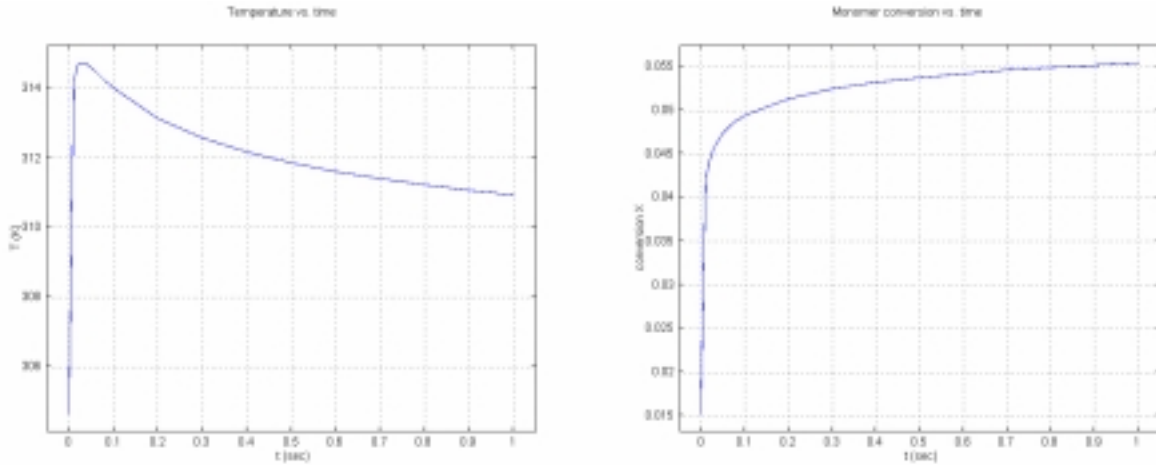


Figure 3 Evolution of temperature and conversion  $\_$  at the line surface center  $(x, 0, 0)$

### Verification and Application

The E4PETeA acrylate with 2wt% DMPA was used to grow single line parts in SLA-250. The parts were elevated out of the resin vat 30min after laser scanning was finished, and drained on the platform for another 15min. The parts were cleaned for 1min in TPM (tri-propylene glycol monomethyl ether) and another 1min in water at room temperature using a Branson 5210 cleaning system in ultra-sonic mode. The parts were dried using compressed air and frozen in liquid nitrogen for 45sec in order to easily break to expose the cross section. The parts were then measured by SEM (scanning electron microscope, Hitachi S800 FEG). Figure 4 shows a picture and dimensions of the cross section of a single line built at a laser scanning speed  $v_s = 0.466$ in/sec. It should be mentioned that specifically how to prepare a part is not important; it is important that different sets of parts (e.g. at different scanning speeds) be built following the same steps (both building and especially postprocessing) in order not to disturb the predictability of the cure process model.

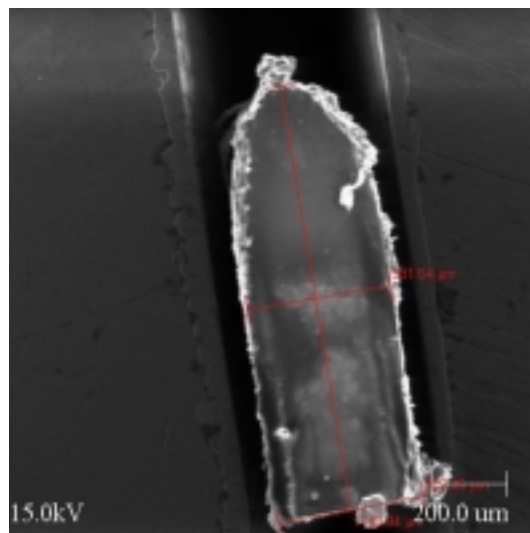


Figure 4 SEM picture of the cross section of single line part built at  $v_s=0.466$ in/sec in SLA-250



From the simulation results in the previous section, Figure 5 shows monomer conversions at different positions in a single line at time = 1s. If we connect the conversion with the cured shape, a contour line with certain conversion corresponds to half of the cured line cross section. Recall the earlier simulation used  $v_s = 0.0272\text{m/sec}$  (1.071in/sec, Table 1). At this drawing speed,  $876.75\mu\text{m}$  and  $312.13\mu\text{m}$  were found to be the maximum depth and maximum width of the cured line as a result of building and measuring about 20 parts. The 90% confidence limits are  $876.75\pm 9.28\mu\text{m}$  and  $312.13\pm 3.67\mu\text{m}$ , respectively. Referring to the conversion contour below, this corresponds to  $3\pm 0.1\%$  conversion at time = 1s. A degree of cure (DOC) threshold model is thus proposed. It takes reaction, mass diffusion, and heat transfer into account, unlike the exposure threshold model which only considers the exposure the resin receives.

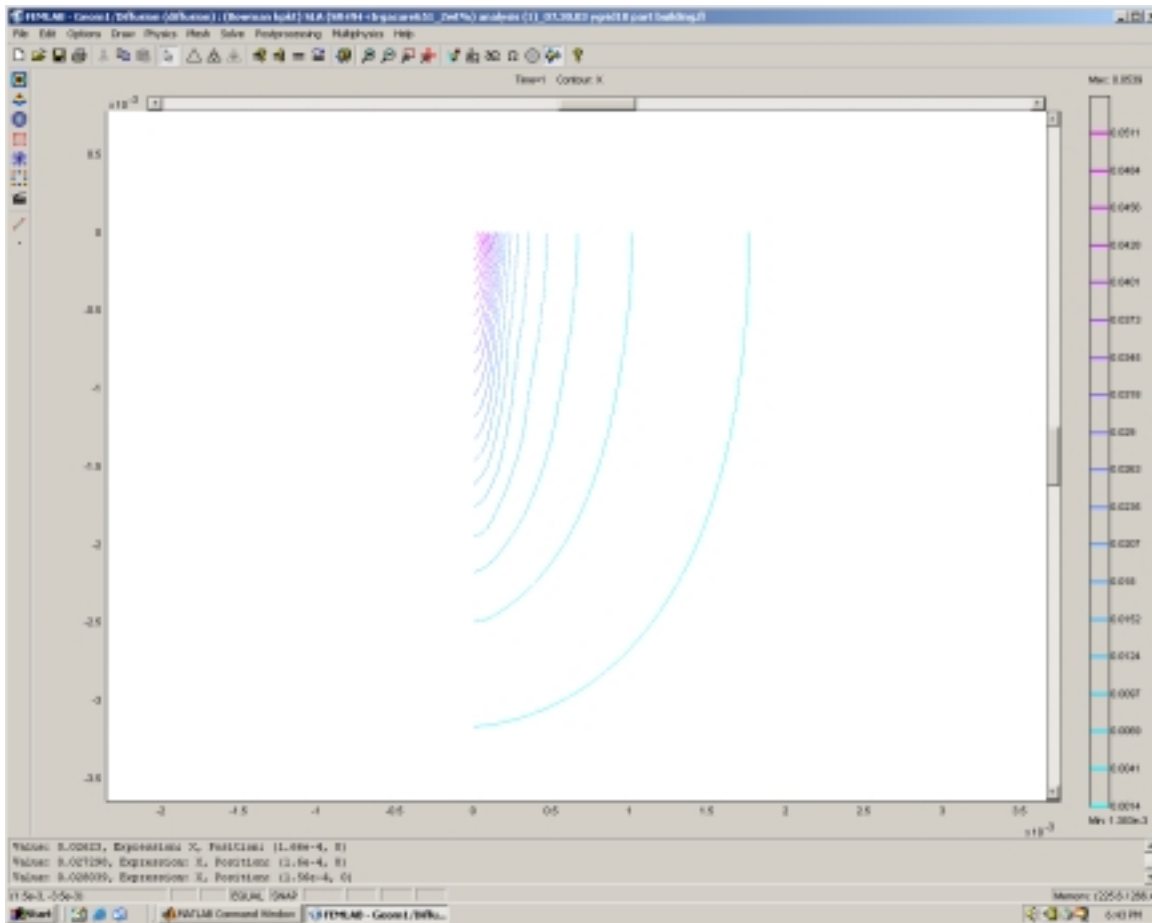


Figure 5 Monomer conversion (X) contour at time = 1s for parts built at  $v_s = 1.071\text{in/sec}$

In the conversion contour plot for the single line part built at  $v_s = 0.466\text{in/sec}$ , the cured conversion line (3% conversion line) corresponds to a maximum depth of  $1050\mu\text{m}$  and maximum half width of  $162.5\mu\text{m}$ . This is in good agreement with the part building results with less than 15% deviation (Table 2). The ability of the SL cure process model to predict the cured shape and size is a good verification and application of the model. The less prediction accuracy in the line width than the cure depth is probably due to the inappropriate assumption of Gaussian laser beam intensity distribution.

Table 2 Correspondence of monomer conversion to the size of cured lines

<b>vs=1.071 in/s</b>	X	depth(μm)	relative error(%)	X	half width(μm)	relative error(%)
Xc model	0.0297	870	<b>0.77</b>	0.0296	148	<b>5.16</b>
experiment	mean	876.75		mean	156.06	
Ec model		1111.06	<b>26.73</b>		167.52	<b>7.34</b>
<b>vs=0.466 in/s</b>	X	depth(μm)	relative error(%)	X	half width(μm)	relative error(%)
Xc model	0.0294	1090		0.0293	166	
	0.0309	1010		0.0308	159	
	average	1050	<b>6.77</b>	average	162.5	<b>14.29</b>
experiment	mean	1126.29		mean	189.6	
Ec model		1310.38	<b>16.35</b>		181.93	<b>4.05</b>

\*model material system: E4PETeA and 2wt% DMPA

For comparison, the WINDOWPANE™ experiments [2] were conducted and  $E_c$  and  $D_p$  of the model acrylate resin were found to be  $7.22\text{mJ/cm}^2$  and  $9.43\text{mils}$ , respectively. The exposure threshold model was then used to predict the cure depth and the prediction error turned out to be within 30% (Table 2). On the other hand, it can predict the full width of the laser cured line more accurately (within 10% error).

From Table 2, it also can be seen that when the laser scanning speed decreases by ~60%, the cure depth increases by ~30%. The sensitivity analysis of model parameters demonstrates that laser scanning speed is not the most sensitive parameter. SL bath temperature, photoinitiator absorptivity and concentration are the factors that affect the SL fabrication results most. Either an increase of the photoinitiator absorptivity or photoinitiator concentration leads to more light absorption, less penetration depth and, therefore, less depth of the reacted monomer (5% less if the parameter increases by 10%). An increase of bath temperature causes a higher reaction rate, more monomer consumed and wider and deeper cured shape. The laser parameters such as laser power, wavelength and beam radius as well as the material properties such as thermal conductivity, heat capacity, heat of polymerization, and quantum yield affect the built part shape and strength, but are not significant. The magnitude of the diffusion coefficient is small for both monomer and radicals in the curing process, but it cannot be taken as zero for the monomer. The presence of monomer diffusion enlarges the cured shape to some degree. The diffusion coefficient for chain radicals is much smaller than that of monomer, and does not have a noticeable effect on the SL process.

## Conclusions

An analytical model of SL resin cure involving heat conduction and diffusion has been presented in this paper. A comprehensive kinetic model was parameterized for a model photosensitive material system (ethoxylated (4) pentaerythritol tetraacrylate with 2,2-dimethoxy-2-phenylacetophenone). Its thermal properties and other physical properties were characterized. Simulations using FEMLAB were conducted to determine the time-dependent distributions of temperature, monomer and radical concentrations, and degree of cure. A critical degree of cure was found and a DOC threshold model was proposed which can predict the part dimensions within 15% error, comparing with 30% prediction error by the exposure threshold model. The degree of cure distribution in the curing process is explored as a “dictionary” to look up the

cured line size or shape upon variation of part building conditions or other related material properties.

A more significant benefit from the “dictionary” is that the process variables that have a significant effect on SL resolution and/or speed can be identified. The SL bath temperature, photoinitiator absorptivity and concentration are found to be the most sensitive parameters that affect the SL fabrication results. The sensitive variables will be the focus of further research meant to improve SL process speed and resolution.

### Acknowledgments

We acknowledge the generous support of the Rapid Prototyping & Manufacturing Institute industry sponsors, particularly 3D Systems, DSM Somos, and Huntsman Chemical, in support of this research.

### References

1. Tang, Y., Muzzy, J.D., Henderson, C.L., and Rosen, D.W. (2003) ‘Stereolithography Cure Modeling and Simulation’, in Bártolo P. and Mitchell G. *et al.* (Eds.) *International Conference on Advanced Research in Virtual and Rapid Prototyping*, Leiria: School of Technology and Management.
2. Jacobs, P.F. (1992) *Rapid Prototyping & Manufacturing: Fundamentals of Stereolithography*, Dearborn, MI: Society of Manufacturing Engineers.
3. Flach, L. and Chartoff, R.P. (1995) ‘A Process Model for Nonisothermal Photopolymerization with a Laser Light Source. I: Basic Model Development’, *Polymer Engineering and Science*, Vol. 35, pp.483-492.
4. Goodner, M.D., Lee, H.R., and Bowman, C.N. (1997) ‘Method for Determining the Kinetic Parameters in Diffusion-controlled Free-Radical Homopolymerizations’, *Ind. Eng. Chem. Res.*, Vol.36, pp.1247-1252.
5. Goodner, M.D. and Bowman, C.N. (2002) ‘Development of Comprehensive Free Radical Photopolymerization Model Incorporating Heat and Mass Transfer Effects in Thick Films’, *Chemical Engineering Science*, Vol.57, pp.887-900.
6. Anseth, K.S., Wang, C.M., and Bowman, C.N. (1994) ‘Reaction Behaviour and Kinetic Constants for Photopolymerizations of Multi(meth)acrylate Monomers’, *Polymer*, Vol.35, pp.3243-3250.
7. Pananakis, D. and Watts, D.C. (2000) ‘Incorporation of the Heating Effect of the Light Source in a Non-isothermal Model of a Visible-light-cured Resin Composites’, *J. Mat. Sci.*, Vol.35, pp.4589-4600.
8. Cussler, E.L. (1997) *Diffusion: Mass Transfer in Fluid Systems*, New York: Cambridge University Press.
9. SR-494 data sheet, <http://www.sartomer.com/>
10. Steinmann, B. *et al.* (1995) ‘Photosensitive Compositions’, *United States Patent*, Pat. No. 5,476,748.
11. Steinmann, B. *et al.* (1999) ‘Liquid, Radiation-curable Composition, Especially for Stereolithography’, *United States Patent*, Pat. No. 5,972,563.

12. Pang, T.H. *et al.* (2000) 'Liquid Radiation-curable Composition Especially for Producing Cured Articles by Stereolithography having High Heat Deflection Temperatures', *United States Patent*, Pat. No. 6,100,007.
13. Melisaris, A.P. *et al.* (2000) 'Liquid, Radiation-curable Composition, Especially for Producing Flexible Cured Articles by Stereolithography', *United States Patent*, Pat. No. 6,136,497.
14. Tryson, G.R. and Shultz A.R. (1979) 'A Calorimetric Study of Acrylate Photopolymerization', *J. of Poly. Sci.: Poly. Phys. Ed.*, Vol.17, pp.2059-2075.
15. Mateo, J.L., Serrano, J., and Bosch, P. (1997), 'Photopolymerization of Di- and Tetrafunctional Methacrylic Monomers in a Polymeric Medium: Kinetics and Evidence of Reaction Diffusion throughout the Photopolymerization Reaction', *Macromolecules*, Vol.30, pp.1285-1288.
16. COMSOL Group, <http://www.comsol.com/>
17. Tang, Y., Henderson, C.L., Muzzy, J.D., and Rosen, D.W. (2004) 'Stereolithography Cure Modeling and Simulation', *Int. J. Materials and Product Technology*, Vol.21, pp.255-272.